



In Silico Analysis for Exploring the Potential Inhibitors Against Breast Cancer (MCF7) Using Curcumin Analogue Compounds

Neni Frimayanti ^{1,*}, Adel Zamri ², Yum Eryanti ²

¹ Sekolah Tinggi Ilmu Farmasi (STIFAR), Pekanbaru, Riau, Indonesia

² Department of Chemistry, Faculty of Mathematics and Natural Sciences, Universitas Riau, Riau, 28293, Indonesia

* Corresponding author: nenifrimayanti@gmail.com

<https://doi.org/10.14710/jksa.27.6.250-257>



Article Info

Article history:

Received: 10th October 2023

Revised: 22nd May 2024

Accepted: 22nd May 2024

Online: 30th June 2024

Keywords:

curcumin; docking; molecular dynamic; pharmacophore; QSAR

Abstract

Breast cancer is one of the most problematic diseases in the world. Currently, there are no potential vaccines for the treatment of this disease. Therefore, finding effective compounds, such as curcumin analogues, is crucial to inhibit breast cancer. Forty-five synthesized curcumin analogues were tested on the MCF7 cell line using the MTT assay. It was shown that nine curcumin compounds, Cpd 5, Cpd 9, Cpd 17, Cpd 18, Cpd 21, Cpd 25, Cpd 28, Cpd 32, and Cpd 45, had better inhibitory activities against breast cancer. Furthermore, *in silico* analysis was developed using 2D and 3D QSAR models with high predictive ability, with an r^2 value of 0.834. In addition, based on molecular docking, molecular dynamics, and pharmacophore results, it was shown that these nine compounds had the lowest binding free energy and were also stable during the simulation. The presence of methoxy groups, hydrogen bond donors, and aromatic ring features are the main factors that enhance the biological activity of curcumin analogues. Therefore, these compounds could serve as references for the next stage of drug design.

1. Introduction

Cancer is one of the most severe diseases and the leading cause of death. Nearly 10 million deaths and 19.3 million new cases are estimated by 2020 [1]. Breast cancer is one of the most dangerous types of cancer. Breast cancer is one of the leading causes of death in women worldwide. Due to the absence of potential vaccines to prevent this disease, patients diagnosed with cancer normally choose chemotherapy as an effective treatment to suppress tumor growth. Many chemotherapy regimens have been successfully used to treat breast cancer despite the many side effects that accompany it [2].

Curcumin is a derivative of turmeric secondary metabolites with numerous biological properties. It is one of the most commonly used and well-researched multi-targeting phytochemicals against various cancers. In the last decade, some investigations have been conducted on the synthetic modifications of curcumin, especially for breast cancer inhibitors. With a five-thousand-year history, curcumin, a well-known chemopreventive drug, has been derived from turmeric [3, 4].

In recent years, curcumin has been shown to diminish the invasion and migration of various malignant cancer cell types, induce apoptotic and non-apoptotic (autophagocytosis and paraptosis) cell death, and suppress proliferation and survival [5, 6]. Curcumin induces a high level of apoptosis in human breast cancer cells by controlling the expression of genes linked to programmed cell death [7]. Nevertheless, little research has been conducted to investigate the underlying mechanisms of curcumin as a possible treatment for breast cancer.

In silico studies play an essential role in drug design [8]. Recently, some *in silico* studies have been carried out to discover new potential breast cancer inhibitors of curcumin and its derivatives [9] or curcumin and its analogues [10]. However, reports on discovering breast cancer inhibitors using entirely *in silico* tools such as 2D and 3D QSAR, pharmacophores, molecular docking, molecular dynamics (MD), and ADME calculations are limited. Thus, this study uses a computational approach to search for curcumin derivative compounds as new inhibitors for breast cancer MCF7.

2. Experimental

2.1. Synthesis and Biological Testing of Curcumin Analogue

Forty-five curcumin analogues have been synthesized following the procedures outlined in our previous research using base- or acid-catalyzed aldol condensation reactions of the appropriately substituted benzaldehyde and corresponding NH-4-piperidones, N-methyl-4-piperidones, and N-benzyl-4-piperidones [11, 12]. The biological activity was determined, and MCF-7 cells were seeded into 96-well plates at an initial cell density of approximately 3×10^4 cells cm^{-3} . After 24 h of incubation for cell attachment and growth, various concentrations of the samples were added. First, the compounds were dissolved in DMSO at the required concentration. Subsequently, six desirable concentrations were prepared using PBS (phosphoric buffer solution at pH = 7.30–7.65).

Control wells were treated with DMSO alone. The assay was terminated after a 48 h incubation period by adding MTT reagent [3-(4,5-dimethylthiazol-2-yl)-2,5-diphenyl tetrazolium bromide; also named thiazol blue], and the incubation was continued for another 4 h, in which the MTT-stop solution containing SDS (sodium dodecyl sulfate) was added and another 24 h incubation was conducted. The optical density was measured using a microplate reader at 550 nm. The IC_{50} values were obtained from the plotted graph of the percentage of live cells compared to the control (%), receiving only PBS and DMSO, versus the tested concentration of compounds (μM). The IC_{50} value is the concentration required for a 50% growth inhibition. Each assay and analysis was performed in triplicate and averaged. The cytotoxic activity of the isolated compounds 1–4 was evaluated against the MCF-7 breast cancer cells according to a method described [13], and cisplatin (IC_{50} 27.0 μM) was used as a positive control [14].

2.2. 2D QSAR Model

As presented in Table S.1, the 45 curcumin analogues and their biological activity values (IC_{50}) were divided into a training set for QSAR model development and a test set for model validation. 2D QSAR is a powerful tool for explaining the relationship between the chemical structure performed by first sorting through the list of biological activities in the increasing and experimental observations. The 2D QSAR model was started by sketching the 2D molecular structure of curcumin using ChemDraw 15, then conversing into a 3D structure using

ChemBio 3D Ultra. Following that, energy minimization was calculated using the MM2 force field. A set of molecular descriptors was generated using the ChemDes software package [15]. However, not all of these descriptors were used for QSAR model development.

A correlation matrix was used to eliminate highly correlated descriptors. Scaling descriptors were then applied because there may be an underlying relationship between these descriptors. The selected descriptors were then used to build the QSAR model, and a multiple linear regression analysis (MLRA) was performed to develop the QSAR model.

2.3. 3D QSAR Model and Pharmacophore Generation

All compounds in the dataset consisting of 45 curcumin analogues were used to generate a 3D QSAR model using the partial least squares (PLS) technique. The energy of each molecular structure was minimized using MMFF94x force field to a gradient of 0.00001 kcal/mol/Å. Descriptors of these compounds were generated, and simultaneously, pharmacophores of the ligands were constructed. This study generated the best alignment of pharmacophores using two features: hydrogen bond donors and hydrophobic properties. These pharmacophore features were then used to confirm that the 3D-QSAR model could be used to predict the biological activity of unknown compounds and to ensure the applicability of 3D-QSAR using the same properties as the pharmacophore alignment.

2.4. Molecular Docking and Molecular Dynamic

Some compounds showed better activity in the *in vitro* assay, including compounds 5, 9, 17, 18, 21, 25, 28, 32, and 45. These compounds were selected as ligands for docking into proteins. Protein preparation began by downloading the protein tyrosine kinase structure from the Protein Data Bank with PDB ID 1T46. Crystal water molecules were then removed, and alpha carbon and backbone atoms of the protein were energy-minimized. The amino acid residues that interacted with the original ligand were observed and preserved in a two-dimensional representation. QuickPrep tools (MOE 2020.0901) were used for protein preparation. Site Finder was used to determine the active site of the protein. Native ligands from the protein must be re-docked; this process was performed with the placement and refinement of 50 and 10, respectively. The re-docked ligand poses with an RMSD value of less than 2 Å and has the most similar interaction between the re-docked ligand and the native ligand was chosen as the best pose.

Table 1. The statistical output of the QSAR model

Statistical output	Value
Non-cross-validated (r^2)	0.83
Cross-validation (r^2 (CV))	0.79
F-value	26.46
F-probability	1.45e-006
Standard error of estimate (SEE)	0.27
Residual sum of squares (RSS)	0.78
Predictive sum of squares (PRESS)	2.60

Table 2. Calculated value of IC₅₀ of curcumin-based compounds in the test set based on 2D QSAR model

Entry	Compound	Experimental IC ₅₀	Predicted IC ₅₀
1	Cpd 1	14.25	15.01
2	Cpd 6	19.49	19.89
3	Cpd 7	27.54	26.78
4	Cpd 20	44.69	45.00
5	Cpd 24	38.84	38.93
6	Cpd 27	63.00	63.26
7	Cpd 30	32.32	32.68
8	Cpd 37	69.00	69.34
9	Cpd 42	56.11	56.98
10	Cpd 43	60.63	61.01
11	Cpd 44	54.18	55.23
12	Cpd 26	13.34	13.98
13	Cpd 29	17.03	17.89
14	Cpd 23	14.26	14.98
15	Cpd 20	44.69	45.00

Table 3. Calculated value of IC₅₀ of curcumin-based compounds in the test set based on 3D QSAR model

Entry	Compound	Experimental IC ₅₀	Predicted IC ₅₀
1	Cpd 1	14.25	14.76
2	Cpd 6	19.49	18.97
3	Cpd 7	27.54	27.53
4	Cpd 20	44.69	44.98
5	Cpd 24	38.84	38.99
6	Cpd 27	63.00	63.03
7	Cpd 30	32.32	32.89
8	Cpd 37	69.00	69.45
9	Cpd 42	56.11	57.89
10	Cpd 43	60.63	62.23
11	Cpd 44	54.18	53.23
12	Cpd 26	13.34	13.98
13	Cpd 29	17.03	17.89
14	Cpd 23	14.26	14.77
15	Cpd 20	44.69	43.29

Molecular dynamics simulation (i.e., preliminary study) was performed using NAMD (Nanoscale Molecular Dynamics program v.2.9). CHARMM27 (Chemistry at HARvard Macromolecular Mechanics) was utilized as the best-selected force field. The modeled protein was obtained using the TIP3P water box with 2.5 Å water layers for each direction of the coordinated structure. The system was gradually heated using the NVT ensemble from 0 to 300 K over 100 ps. MD simulations were performed on a 50 ns time scale for each system in an isothermal isobaric ensemble (NPT) with periodic boundary conditions. Temperature and pressure parameters were coupled at a rate of one ps. When sampling, the coordinates were recorded every 0.1 ps. The simulations generated the conformations, which were used for further binding free energy calculations and decomposition.

2.5. Adsorption, Distribution, Metabolism, and Excretion (ADME)

The drug-likeness of the potential candidates for breast cancer inhibitors and their physiochemical and pharmacokinetic properties were predicted using ADME profiles. In this study, the ADME profiles were performed and calculated using the SwissADME server (<http://www.swissadme.ch/index.php>).

3. Results and Discussion

3.1. The 2D QSAR Model

The QSAR model was developed using descriptors as the independent variables and biological activity as the dependent variable. The statistical output of the QSAR model is presented in Table 1, and the best QSAR model is presented in Equation (1).

$$Y = 0.5643 * MREF - 0.4375 * MW - 1.6720 * LDI + 0.6879 * nhyd + 0.5435 \quad (1)$$

where, MREF stands for molar refractivity, MW is molecular weight, LDI is the local dipole index, and nhyd is the count of hydrogen bonds.

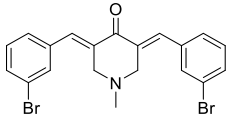
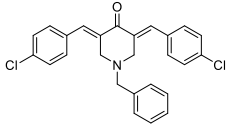
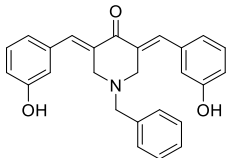
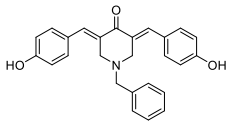
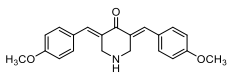
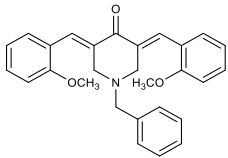
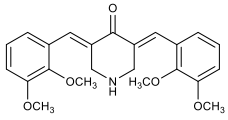
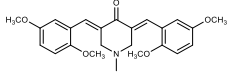
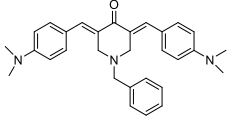
The cross-validated coefficient (r^2 (CV)) is the goodness of prediction, the non-cross-validated conventional correlation coefficient (r^2) is the goodness of fit of the QSAR model, and the F -value defines the degree of statistical confidence. Generally, the QSAR model is acceptable, with r^2 greater than 0.6 and r^2 (CV) greater than 0.5. In this study, the QSAR model had an r^2 of 0.83 and an r^2 (CV) of 0.79. This indicates that the QSAR model is stable and can be used to predict the unknown compounds in the test set. This QSAR model showed that biological activity would improve with increasing molecular refractivity and the number of hydrogen donors (i.e., MREF and nhyd). In addition, the hydrophobic descriptors (that is LDI and W) are also important, and they define the hydrophobic influence of substituents in the interactions of organic compounds with the receptor [16].

The biological activity of compounds in the test set was then predicted using the QSAR model (Equation 1), as listed in Table 2. A correlation coefficient (r^2) of 0.86 was obtained between the predicted and experimental values for the QSAR model.

3.2. 3D QSAR Model and Pharmacophore Generation

The 3D QSAR model consisted of two variables: biological activity was used as the dependent variable, and pharmacophore was the independent variable. The PLS QSAR model was then generated with coefficient correlation (r^2) and root mean square of 0.70 and 0.26, respectively. The validity of this QSAR model was used to ensure the predicted biological activities of compounds that were not considered for building the QSAR model (test set). The predicted and actual values of the test set compounds are listed in Table 3.

Table 4. Docking results

Cpd number	Compound	Residue	RMSD	Binding free energy (kcal/mol)
5		Asp792, Tyr823, Asp810, Glu640, Val643, Gly812	0.00	-43.23
9		Asp810, Glu640, Cys809, Val643, Ile571, Tyr570, His790, Ile789, Tyr570,	0.00	-36.13
17		Glu640, Ala636, Asp810, Asp792, Pro832, Pro791,	0.00	-32.23
18		Arg791, Asp792, His790, Asp810	0.00	-42.20
21		Glu640, Cys809, Asp810, Arg791, His790	0.00	-23.45
25		Thr632, Glu633, Ala636, Leu813, Gly812, Val640, Arg791, His790	0.00	-52.81
28		Asn828, Ala829, Leu831, Gly812, Arg791, Asp810, Glu640	0.00	-32.46
32		Thr632, Leu813, Glu640, Gly812, Arg791, His790, Ile789	0.00	-25.67
45		Thr632, Ala636, Glu633, Glu640, Arg791, Asp810, Gly812, Ile817, Lys818	0.00	-34.34

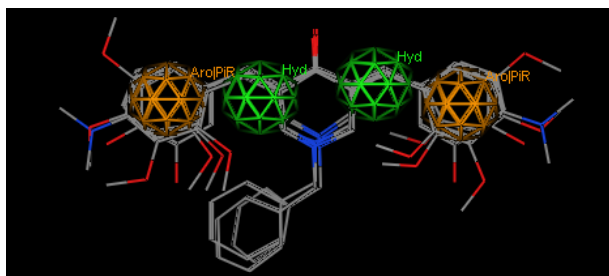


Figure 1. The best pharmacophore hypothesis for curcumin analogue. Pharmacophores are color-coded with orange for the aromatic ring and green for the hydrophobic

The suggested descriptors in the 3D QSAR model were then validated using pharmacophore alignment. The best pharmacophore hypothesis is generated by the hydrophobic sphere (green) and aromatic sphere

(orange). These pharmacophores were considered the key elements contributing to the ligand activity [17, 18]. Figure 1 depicts the pharmacophore hypothesis for the curcumin analogue. It shows the importance of the hydrophobic and aromatic ring features that can enhance breast cancer inhibitory activity [19].

3.3. Molecular Docking

Docking and MD analyses were performed on the active compounds (Cpd 5, 9, 17, 18, 21, 25, 28, 32, and 45). The docking aims to ensure that the active compounds bind well to important residues in the protein active site [20]. Doxorubicin was used as the positive control and was previously docked [21]. The best poses from the docking results were selected based on the lowest docking energy values. The docking results are presented in Table 4.

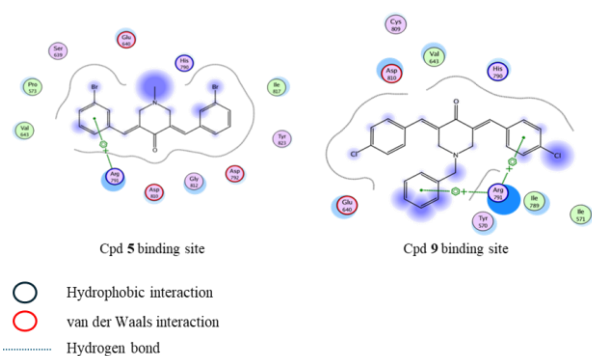


Figure 2. The binding interactions of Cpd 5 and Cpd 9

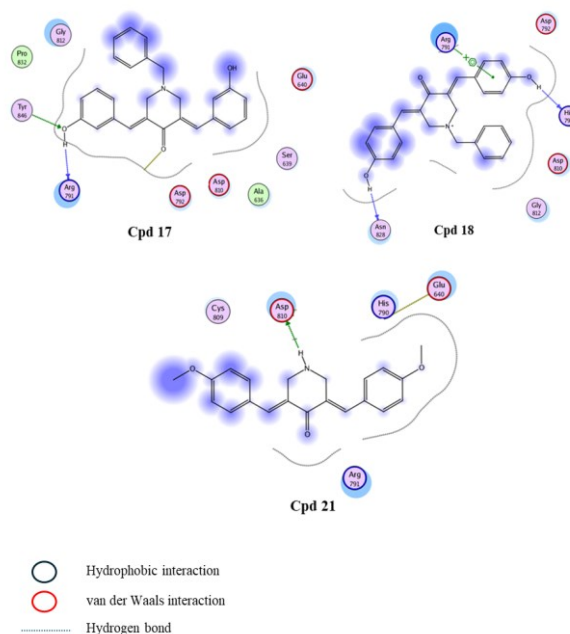


Figure 3. The binding interactions of Cpd 17, Cpd 18, and Cpd 21

Based on their biological activity, Cpd 5 appears to be an active compound. Cpd 5 showed two van der Waals interactions with Glu640 and Asp810. This compound also interacts via π interactions with His790. Another compound that was assumed to be active is Cpd 9. Compound 9 showed to have π interactions with His790 and Arg791. In addition, Glu640 and Asp810 interact with the ligand through van der Waals interactions. Hydrophobic interactions were also observed between the ligand and residue Arg791. The docking results for these compounds are depicted in Figure 2.

Similarly, Cpd 17 was also shown to be an active compound. Hydrogen bonding (dashed blue line) was formed between the hydroxyl group in the ligand and Arg791. Van der Waals interactions with important residues such as Glu640 and Asp810 were also observed. For Cpd 18, hydrogen bonding (dashed blue line) was observed between His790 and the hydroxyl group of the ligand. In addition, van der Waals interactions were constructed between the ligand and residue Asp810, and π interactions were observed with residue Arg791. Van der Waals interactions between Cpd 21 and the residues Glu640 and Asp810 were observed. The binding interaction of Cpd 17, Cpd 18, and Cpd 21 are illustrated in Figure 3.

Cpd 25 showed one hydrogen bond (dashed blue line) with the residue Arg791. In addition, this ligand also showed van der Waals interactions with Glu640 and Asp810. Residues Lys623, His790, and Arg791 interacted with the ligand through π interaction (blue circle). This may explain why this ligand is an active compound. Cpd 28, Cpd 32, and Cpd 45 interact with residues Glu640 and Asp810 through van der Waals and hydrophobic interactions with residue Arg791. The binding interaction of Cpd 25, Cpd 28, Cpd 32, and Cpd 45 with the protein are shown in Figure 4.

Table 5. Interaction with amino acid after MD simulation

Cpd number	Interaction after simulation	Hydrogen bond distance (Å)
5	Asp792, Tyr823, Asp810 , Glu640 , Val643, Gly812	2.9
9	Asp810 , Glu640 , Cys809, Val643, Ile571, Tyr570, His790, Ile789, Tyr570	2.9
17	Glu640 , Ala636, Asp810 , Asp792, Pro832, Pro791	2.9
18	Arg791, Asp792, His790, Asp810	2.9
21	Glu640 , Cys809, Asp810, Arg791, His790	2.9
25	Thr632, Glu633, Ala636, Leu813, Gly812, Val640, Arg791, His790	2.9
28	Asn828, Ala829, Leu831, Gly812, Arg791, Asp810 , Glu640	2.9
32	Thr632, Leu813, Glu640 , Gly812, Arg791, His790, Ile789	2.9
45	Thr632, Ala636, Glu633, Glu640 , Arg791, Asp810 , Gly812, Ile817, Lys818	2.9

Bold: important residue

Table 6. ADME profiles of active compounds

Profile	Cpd 5	Cpd 9	Cpd 17	Cpd 18	Cpd 21	Cpd 25	Cpd 28	Cpd 32	Cpd 45
MW (g/mol)	447.16	434.36	397.47	397.47	335.40	425.52	395.45	409.47	451.60
Consensus Log P _{o/w}	4.76	5.76	3.85	3.84	3.24	4.60	3.15	3.47	4.67
Hydrogen bond donor	1	0	2	2	1	0	1	0	0
Hydrogen bond acceptor	0	2	4	4	4	4	6	6	2
Rotatable bonds	2	4	4	4	4	6	6	6	6
Druglikeness (Lipinski)	Yes	Yes	Yes	Yes	Yes	Yes	Yes	Yes	Yes

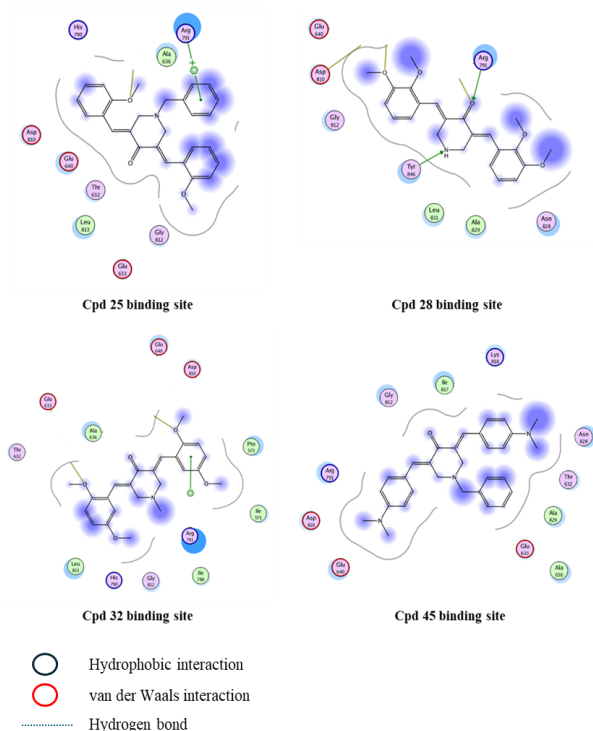


Figure 4. The binding interaction of Cpd 25, Cpd 28, Cpd 32, and Cpd 45 with the protein

3.4. Molecular Dynamics Simulation

Molecular dynamics (MD) simulations have investigated hydrogen bonding interactions and interactions between ligands and proteins [22, 23]. Generally, the conformations of the active ligand are maintained to bind with important residues and are inapplicable to non-active ligands [24], as shown in Figure 5. MD simulations showed that these nine compounds could explore the interactions between the ligand and receptor. The stability of the MD simulation results was used to confirm the ligand-binding profile.

In addition, the stability of MD can also be used to ensure that the interaction between the protein and active compounds is maintained [25]. MD simulation was performed for 50 ns. This process began by employing optimal stability and minimal energy at 300 K to assess how strongly the ligand binds to the binding site. Hydrogen bonding was confirmed for the potential active compounds (specifically, nine compounds) both before and after the MD simulation. RMSD graphs for these compounds are presented in Figure S.2.

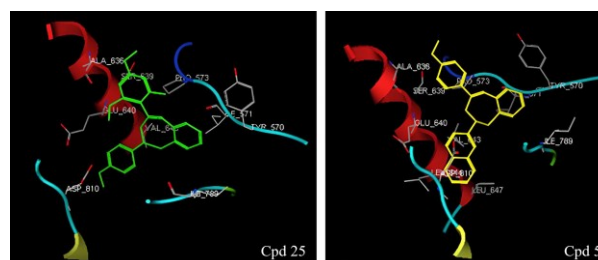


Figure 5. Visualization of the binding mode of the most active compounds Cpd 25 and Cpd 5

Nine of these compounds could bind well with the important residues, Glu640 and Asp810, before and after simulation with a hydrogen bond distance of less than 2.9 Å, which indicated that these compounds could be used as breast cancer inhibitors. A visualization of the MD simulation is shown in Figure 5. Table 5 presents the interactions with the amino acids after the simulation.

3.5. Adsorption, Distribution, Metabolism, Excretion (ADME)

For the promising compounds, i.e., Cpd 5, Cpd 9, Cpd 17, Cpd 18, Cpd 21, Cpd 25, Cpd 28, Cpd 32, and Cpd 45, the pharmacokinetic profile is also needed to conduct. This profile consisted of *in silico* ADME profiling. ADME is expected to reduce the risk of late-stage attrition in drug development [26]. An *in silico* study was performed to predict drug-like molecular properties based on Lipinski's Rule of Five. Lipinski's Rule of Five was calculated to determine the absorption or permeability levels of potential compounds across lipid bilayers in the human body. The results of the ADME calculations for these compounds are presented in Table 6. A compound can be predicted to have good bioavailability if it follows Lipinski's rule (maximum MW is 500, log P is not greater than 5, hydrogen bond donor is less than 5, and hydrogen bond acceptor is less than 10) [27]. Based on the ADME calculation, all active compounds have drug-like properties and can be used as potential inhibitors against breast cancer.

4. Conclusion

2D and 3D QSAR models have been effectively developed, demonstrating strong predictive capabilities. Both types of QSAR models indicate that hydrophobic properties and hydrogen bond donors can amplify the inhibitory activity against breast cancer. Analyses involving docking and molecular dynamics reveal the significance of residues Glu640, Arg791, and Asp810 in

interacting with the compounds. Moreover, a computational approach combined with biological assays has confirmed Cpd 5, 9, 17, 18, 21, 25, 28, 32, and 45 as promising candidates for advancing second-generation drug discovery targeting breast cancer.

Acknowledgment

This article is especially dedicated to the memory of our dear colleague, Prof. Dr. Adel Zamri, MS, DEA.

References

- [1] Amena Ali, Abuzer Ali, Abu Tahir, Md. Afroz Bakht, Salahuddin, Mohamed Jawed Ahsan, Molecular Engineering of Curcumin, an Active Constituent of *Curcuma longa* L. (Turmeric) of the Family *Zingiberaceae* with Improved Antiproliferative Activity, *Plants*, 10, 8, (2021), 1559 <https://doi.org/10.3390/plants10081559>
- [2] Xinqiang Song, Mu Zhang, Erqin Dai, Yuan Luo, Molecular targets of curcumin in breast cancer (Review), *Mol Med Rep*, 19, 1, (2019), 23-29 <https://doi.org/10.3892/mmr.2018.9665>
- [3] Ying-Bo Li, Jian-Li Gao, Zhang-Feng Zhong, Pui-Man Hoi, Simon Ming-Yuen Lee, Yi-Tao Wang, Bisdemethoxycurcumin suppresses MCF-7 cells proliferation by inducing ROS accumulation and modulating senescence-related pathways, *Pharmacological Reports*, 65, 3, (2013), 700-709 [https://doi.org/10.1016/S1734-1140\(13\)71048-X](https://doi.org/10.1016/S1734-1140(13)71048-X)
- [4] Cheppail Ramachandran, Sonia Rodriguez, Reshma Ramachandran, PK Raveendran Nair, Hugo Fonseca, Ziad Khatib, Enrique Escalon, Steven J. Melnick, Expression Profiles of Apoptotic Genes Induced by Curcumin in Human Breast Cancer and Mammary Epithelial Cell Lines, *Anticancer Research*, 25, 5, (2005), 3293-3302
- [5] Purusotam Basnet, Natasa Skalko-Basnet, Curcumin: An Anti-Inflammatory Molecule from a Curry Spice on the Path to Cancer Treatment, *Molecules*, 16, 6, (2011), 4567-4598 <https://doi.org/10.3390/molecules16064567>
- [6] Yan Chen, Wenxiu Shu, Weihua Chen, Qing Wu, Hongli Liu, Guohui Cui, Curcumin, both Histone Deacetylase and p300/CBP-Specific Inhibitor, Represses the Activity of Nuclear Factor Kappa B and Notch 1 in Raji Cells, *Basic & Clinical Pharmacology & Toxicology*, 101, 6, (2007), 427-433 <https://doi.org/10.1111/j.1742-7843.2007.00142.x>
- [7] Ajay Goel, Ajaikumar B. Kunnumakkara, Bharat B. Aggarwal, Curcumin as "Curecumin": From kitchen to clinic, *Biochemical Pharmacology*, 75, 4, (2008), 787-809 <https://doi.org/10.1016/j.bcp.2007.08.016>
- [8] Neni Frimayanti, Ihsan Ikhtiarudin, Rahma Dona, Tiara Tri Agustini, Fri Murdiya, Adel Zamri, A Computational Approach to Drug Discovery: Search for Chalcone Analogues as the Potential Candidates for Anti Colorectal Cancer (HT29), *Walailak Journal of Science and Technology (WJST)*, 17, 2, (2018), 64-74 <https://doi.org/10.48048/wjst.2020.5910>
- [9] Zintle Mbese, Vuyolwethu Khwaza, Blessing Atim Aderibigbe, Curcumin and Its Derivatives as Potential Therapeutic Agents in Prostate, Colon and Breast Cancers, *Molecules*, 24, 23, (2019), 4386 <https://doi.org/10.3390/molecules24234386>
- [10] Fiona C. Rodrigues, N. V. Anil Kumar, Gangadhar Hari, K. S. R. Pai, Goutam Thakur, The inhibitory potency of isoxazole-curcumin analogue for the management of breast cancer: A comparative in vitro and molecular modeling investigation, *Chemical Papers*, 75, (2021), 5995-6008 <https://doi.org/10.1007/s11696-021-01775-9>
- [11] Yum Eryanti, Tati Herlina, Adel Zamri, Siti Nadiah Abdul Halim, Yoshihito Shiono, Yana M. Syah, Khalijah Awang, Unang Supratman, 3,5-Bis(2-hydroxybenzylidene)piperidin-4-one, *Molbank*, 2014, 2, (2014), M825 <https://doi.org/10.3390/M825>
- [12] Yum Eryanti, Adel Zamri, Neni Frimayanti, Hilwan Yuda Teruna, Unang Supratman, Tati Herlina, Yoshihito Shiono, Synthesis, Structure-Activity Relationship, Docking and Molecular Dynamic Simulation of Curcumin Analogues Against HL-60 for Anti Cancer Agents (Leukemia), *Oriental Journal of Chemistry*, 33, 5, (2017), 2164-2172 <http://dx.doi.org/10.13005/ojc/330503>
- [13] Philip Skehan, Ritsa Storeng, Dominic Scudiero, Anne Monks, James McMahon, David Vistica, Jonathan T. Warren, Heidi Bokesch, Susan Kenney, Michael R. Boyd, New Colorimetric Cytotoxicity Assay for Anticancer-Drug Screening, *JNCI: Journal of the National Cancer Institute*, 82, 13, (1990), 1107-1112 <https://doi.org/10.1093/jnci/82.13.1107>
- [14] Yuni Elsa Hadisaputri, Tatsuya Miyazaki, Shigemasa Suzuki, Takehiko Yokobori, Tutomu Kobayashi, Naritaka Tanaka, Takanori Inose, Makoto Sohda, Hiroyuki Kuwano, *TNFAIP8* Overexpression: Clinical Relevance to Esophageal Squamous Cell Carcinoma, *Annals of Surgical Oncology*, 19, (2012), 589-596 <https://doi.org/10.1245/s10434-011-2097-1>
- [15] Jie Dong, Dong-Sheng Cao, Hong-Yu Miao, Shao Liu, Bai-Chuan Deng, Yong-Huan Yun, Ning-Ning Wang, Ai-Ping Lu, Wen-Bin Zeng, Alex F. Chen, ChemDes: an integrated web-based platform for molecular descriptor and fingerprint computation, *Journal of Cheminformatics*, 7, (2015), 60 <https://doi.org/10.1186/s13321-015-0109-z>
- [16] Neni Frimayanti, Vannajan Sanghiran Lee, Sharifuddin M. Zain, Habibah A. Wahab, Noorsaadah Abd. Rahman, 2D, 3D-QSAR, and pharmacophore studies on thiazolidine-4-carboxylic acid derivatives as neuraminidase inhibitors in H3N2 influenza virus, *Medicinal Chemistry Research*, 23, 3, (2014), 1447-1453 <https://doi.org/10.1007/s00044-013-0750-x>
- [17] Madhulata Kumari, Subhash Chandra, Neeraj Tiwari, Naidu Subbarao, 3D QSAR, pharmacophore and molecular docking studies of known inhibitors and designing of novel inhibitors for M18 aspartyl aminopeptidase of *Plasmodium falciparum*, *BMC Structural Biology*, 16, (2016), 12 <https://doi.org/10.1186/s12900-016-0063-7>
- [18] Yongmei Pan, Yanli Wang, Stephen H. Bryant, Pharmacophore and 3D-QSAR Characterization of 6-Arylquinazolin-4-amines as Cdc2-like Kinase 4 (Clk4) and Dual Specificity Tyrosine-phosphorylation-regulated Kinase 1A (Dyrk1A) Inhibitors, *Journal of Chemical Information and Modeling*, 53, 4, (2013), 938-947 <https://doi.org/10.1021/ci300625c>
- [19] Rathinasabapathy Pushpalatha, Subramanian Selvamuthukumar, Duraisamy Kilimozhi,

Comparative Insilico Docking Analysis of Curcumin and Resveratrol on Breast Cancer Proteins and their Synergistic Effect on MCF-7 Cell Line, *Journal of Young Pharmacists*, 9, 4, (2017), 480-485
<https://dx.doi.org/10.5530/jyp.2017.9.94>

- [20] F. Frimayanti, Benni Iskandar, Marzieh Yaeghoobi, Heh Choon Han, Sharifuddin M. Zain, Rohana Yusof, Noorsaadah Abdul Rahman, Docking, synthesis and bioassay studies of imine derivatives as potential inhibitors for dengue NS2B/NS3 serine protease, *Asian Pacific Journal of Tropical Disease*, 7, 12, (2017), 792-796 <https://doi.org/10.12980/apjtd.7.2017D7-177>
- [21] N. Frimayanti, M. Yaeghoobi, I. Ikhtiarudin, D. R. W. Putri, H. Namavar, F. S. Bitaraf, Insight on the In Silico Study and Biological Activity Assay of Chalcone-Based 1, 5-Benzothiazepines as Potential Inhibitor for Breast Cancer MCF7, *Chiang Mai University Journal of Natural Sciences*, 20, 1, (2021), e2021019
<https://doi.org/10.12982/CMUJNS.2021.019>
- [22] Lu Zhou, Jiewei Zhu, Yifan Zhao, Honghe Ma, A molecular dynamics study on thermal conductivity enhancement mechanism of nanofluids – Effect of nanoparticle aggregation, *International Journal of Heat and Mass Transfer*, 183, (2022), 122124
<https://doi.org/10.1016/j.ijheatmasstransfer.2021.122124>
- [23] Belal O. Al-Najjar, Ashok K. Shakya, Fadi G. Saqallah, Rana Said, Pharmacophore modeling and 3D-QSAR studies of 15-hydroxyprostaglandin dehydrogenase (15-PGDH) inhibitors, (2017),
- [24] Maryam Abbasi, Hojjat Sadeghi-Aliabadi, Massoud Amanlou, Prediction of new Hsp90 inhibitors based on 3,4-isoxazolidiamide scaffold using QSAR study, molecular docking and molecular dynamic simulation, *DARU Journal of Pharmaceutical Sciences*, 25, (2017), 17 <https://doi.org/10.1186/s40199-017-0182-0>
- [25] Neni Frimayanti, Marzieh Yaeghoobi, Hamid Namavar, Mashitoh Cindy Utari, Meiriza Djohari, Cindy Oktaviana Laia, In silico analysis approach for screening new agents for breast cancer inhibitors based on 1, 5-benzothiazepine, *Pharmaceutical Sciences Asia*, 49, 5, (2022), 446-453
<https://doi.org/10.29090/psa.2022.05.22.001>
- [26] Fumiyoshi Yamashita, Mitsuru Hashida, In Silico Approaches for Predicting ADME Properties of Drugs, *Drug Metabolism and Pharmacokinetics*, 19, 5, (2004), 327-338
<https://doi.org/10.2133/dmpk.19.327>
- [27] Christopher A. Lipinski, Franco Lombardo, Beryl W. Dominy, Paul J. Feeney, Experimental and computational approaches to estimate solubility and permeability in drug discovery and development settings, *Advanced Drug Delivery Reviews*, 64, (2012), 4-17 <https://doi.org/10.1016/j.addr.2012.09.019>